

Heralded generation of entangled photon pairs

Stefanie Barz^{1,2,†}, Gunther Cronenberg^{1,2†}, Anton Zeilinger^{1,2}, Philip Walther^{1,2}

¹ *Faculty of Physics, University of Vienna, Boltzmannngasse 5, A-1090 Vienna, Austria*

² *Institute for Quantum Optics and Quantum Information (IQOQI),
Austrian Academy of Sciences, Boltzmannngasse 3, A-1090 Vienna, Austria*

[†] *These authors contributed equally to this work*

Entangled photons are a crucial resource for quantum communication and linear optical quantum computation. Unfortunately, the applicability of many photon-based schemes is limited due to the stochastic character of the photon sources. Therefore, a worldwide effort has focused in overcoming the limitation of probabilistic emission by generating two-photon entangled states conditioned on the detection of auxiliary photons. Here we present the first heralded generation of photon states that are maximally entangled in polarization with linear optics and standard photon detection from spontaneous parametric down-conversion [1]. We utilize the down-conversion state corresponding to the generation of three photon pairs, where the coincident detection of four auxiliary photons unambiguously heralds the successful preparation of the entangled state [2]. This controlled generation of entangled photon states is a significant step towards the applicability of a linear optics quantum network, in particular for entanglement swapping, quantum teleportation, quantum cryptography and scalable approaches towards photonics-based quantum computing [3].

Photons are generally accepted as the best candidate for quantum communication due to their lack of decoherence and their possibility of being easily manipulated. However, it has also been discovered that a scalable quantum computer can in principle be realized by using only single-photon sources, linear optical elements and single-photon detectors [4]. Several proof-of-principle demonstrations for linear optical quantum computing have been given, including controlled-NOT gates [5–8], Grover’s search algorithm [9, 10], Deutsch-Josza algorithm [11], Shor’s factorization algorithm [12, 13] and the promising model of the one-way quantum computation [14].

A main issue on the path of photonic quantum information processing is that the best current source for photonic entanglement, spontaneous parametric down-conversion (SPDC), is a process where the photons are created at random times. All photons involved in a protocol need to be measured including a detection of the desired output state. This impedes the applicability of many of the beautiful proof-of-principle experiments, especially when dealing with multiple photon pairs [3] and standard detectors without photon number resolution. Other leading technologies in this effort are based on other physical systems including single trapped atoms and atomic ensembles [15], quantum dots [16], or nitrogen-vacancy centers in diamond [17]. Although these systems are very promising candidates, each of these quantum state emitters faces significant challenges for realizing heralded entangled states; typically due to low coupling efficiencies, the uncertainty in emission time or the distinguishability in frequency of the photons created.

However, the probabilistic nature originating from SPDC can be overcome by several approaches conditioned on the detection of auxiliary photons [2, 18, 19]. It was shown that the production of one heralded polarization-entangled photon pair using only conventional down-conversion sources, linear optical elements, and projective measurements requires at least three entangled pairs [20]. Here we describe an experimental realization for producing heralded two-

photon entanglement along these lines, suggested by Śliwa and Banaszek that relies on triple-pair emission from a single down-conversion source [2]. This scheme shows significant advantages compared to other schemes where either several SPDC sources and two-qubit logic gates [18] or more ancilla photons [19] are required.

Current down-conversion experiments allow for the simultaneous generation of three photon pairs [21–24] with typical detection count rates, dependent on the experimental configuration, of about 10^{-3} to 10^{-1} Hz. We use a setup of this kind such that the coincident detection of four auxiliary photons is used to predict the presence of two polarization-entangled photons in the output modes. The auxiliary photons thus herald the presence of a Bell state and it is not necessary to perform a measurement on that state to confirm its presence.

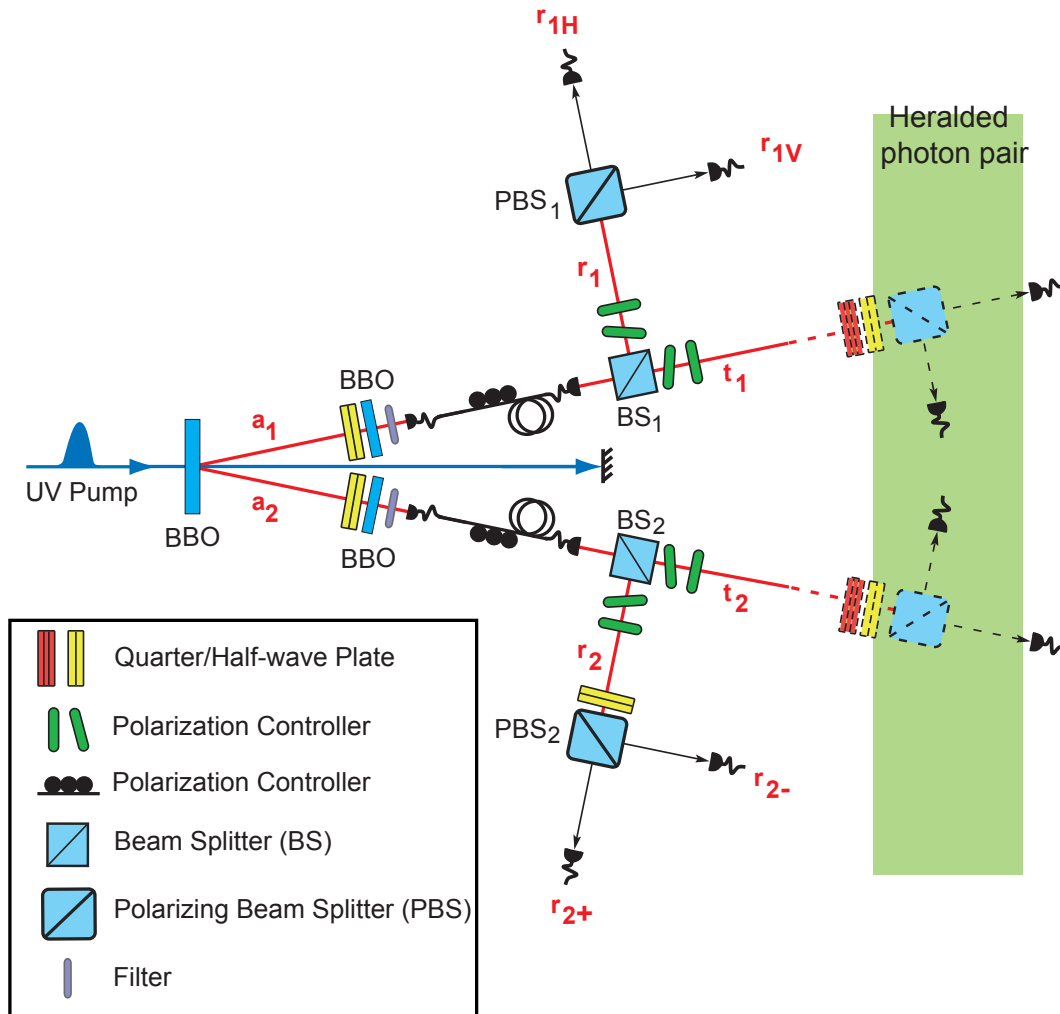


FIG. 1: Setup for the heralded generation of entangled photon pairs. Six photons are created simultaneously by exploiting higher-order emissions in a spontaneous parametric down-conversion process. The photons are passing a narrowband filter and are coupled to single-mode fibers. They are brought to beam splitters and the reflected modes are analyzed in $|H/V\rangle$ basis and in $|\pm\rangle$ basis, respectively, using polarizing beam splitters (PBS) and a half-wave plate (HWP) orientated at 45° . State characterization of the heralded photon pair in the transmitted modes is performed via polarization analysis and the help of quarter-wave plates (QWPs), HWPs and PBSs.

Figure 1 gives a schematic diagram of our setup to generate the heralded state $|\phi^+\rangle = \frac{1}{\sqrt{2}}(|H\rangle_{t_1}|H\rangle_{t_2} + |V\rangle_{t_1}|V\rangle_{t_2})$, where H and V denote horizontal and vertical polarization, respectively, whereas t_1 and t_2 correspond to the transmitted modes after the beam splitters. For generating the heralded state, $|\phi^+\rangle$, three photon pairs have to be emitted simultaneously into spatial modes a_1 and a_2 , resulting in:

$$|\Psi_3\rangle = 1/2 \cdot (|HHH\rangle_{a_1}|VVV\rangle_{a_2} - |HHV\rangle_{a_1}|VVH\rangle_{a_2} + |V VH\rangle_{a_1}|HHV\rangle_{a_2} - |VVV\rangle_{a_1}|HHH\rangle_{a_2})$$

These photons are guided to non-polarizing beam splitters (BS_1 and BS_2) with various splitting ratios. Our scheme only succeeds when four photons are reflected and measured in a four-fold coincidence. The two reflected photons of BS_1 are projected onto $|H/V\rangle$ basis for mode r_1 , while the two reflected photons of BS_2 are measured in $|\pm\rangle = \frac{1}{\sqrt{2}}(|H\rangle \pm |V\rangle)$ basis for mode r_2 . We are interested in the case where one photon is present in each of the modes $r_{1H,1V}$ and $r_{2+,2-}$. Considering only these terms, the output state results in

$$|\Psi_3\rangle = C(\theta_1, \theta_2) \cdot |H\rangle_{r_{1H}}|V\rangle_{r_{1V}}|+\rangle_{r_{2+}}|-\rangle_{r_{2-}} \cdot \frac{1}{\sqrt{2}}(|H\rangle_{t_1}|H\rangle_{t_2} + |V\rangle_{t_1}|V\rangle_{t_2}) \quad (1)$$

where $C(\theta_1, \theta_2)$ is a constant depending on the transmission coefficients of the beam splitters. The coincident detection of one and only one photon in the modes r_{1H} , r_{1V} , r_{2+} and r_{2-} heralds the presence of an entangled photon pair in state $|\phi^+\rangle$ in the output modes t_1, t_2 . In the present scheme such a case can only be achieved by three-pair emission from SPDC. The contribution from two-pair emission is suppressed by destructive quantum interference in the HWP rotation used for $r_{2+,2-}$. This quantum interference together with the use of number-resolving detectors ensures that the remaining two photons are found in the transmitted modes. If a high transmission of the beam splitters is chosen, it still can be assumed with high probability that the two photons are transmitted even without the use of number-resolving detectors.

In our case of using standard detectors (PerkinElmer photo-avalanche diodes) the transmission of the non-polarizing beam splitters should ideally be as high as possible such that a measured four-photon coincidence corresponds to precisely four photons and thus heralds our desired state. Therefore for demonstrating this dependency we choose beam splitters with different transmission rates of 17%, 50% and 70%. Obviously the disadvantage of increasing the probability of heralding a $|\phi^+\rangle$ state - which in principle can be approximately unity - is a reduction in the four-fold coincidence rate for triggering this state. Only the recent improvements of laser sources enable stable UV beams with sufficient power for keeping the measurement time reasonable; in our case the typical counting time for one measurement setting varies from 24h to 72h. The actual rate R of the four-fold coincidences is about $R_{17/83} = 83$, $R_{50/50} = 14$ and $R_{70/30} = 0.4$ per minute.

For characterizing our heralded state, all polarization-dependent measurement outcomes in the output modes t_1 and t_2 that are triggered by the four-fold coincidence in modes r_{1H} , r_{1V} , r_{2+} , and r_{2-} are analyzed as a function of the beam splitter transmission. The measured probabilities of finding the various photon numbers in the output modes are shown in Table I and allow for the reconstruction of the diagonal elements of the density matrix in the photon number basis $|n_1\rangle_{t_1}|n_2\rangle_{t_2}$, where n_1 and n_2 are the Fock or photon-number states per spatial mode (see Supplementary Information). The dependency of the photon-number statistic on the beam splitter ratio can be clearly seen as the vacuum contribution $P_{0,0}$ decreases with higher transmission rates. The resulting probability of heralded entanglement generation is graphically shown in Figure 2 as a function of the beam splitter transmission.

	17/83	30/70	50/50	70/30
$P_{0;0}$	$(9.74 \pm 0.002) \cdot 10^{-1}$	$(9.63 \pm 0.003) \cdot 10^{-1}$	$(9.15 \pm 0.006) \cdot 10^{-1}$	$(8.68 \pm 0.02) \cdot 10^{-1}$
$P_{1;0} + P_{0;1}$	$(2.57 \pm 0.02) \cdot 10^{-2}$	$(3.67 \pm 0.03) \cdot 10^{-2}$	$(8.19 \pm 0.06) \cdot 10^{-2}$	$(1.23 \pm 0.03) \cdot 10^{-1}$
$P_{1;1}$	$(2.58 \pm 0.16) \cdot 10^{-4}$	$(6.14 \pm 0.35) \cdot 10^{-4}$	$(3.06 \pm 0.13) \cdot 10^{-3}$	$(8.03 \pm 0.65) \cdot 10^{-3}$
$P_{2;0} + P_{0;2}$	$(2.75 \pm 0.51) \cdot 10^{-5}$	$(3.57 \pm 0.84) \cdot 10^{-5}$	$(3.72 \pm 0.36) \cdot 10^{-4}$	$(7.49 \pm 0.14) \cdot 10^{-4}$
$P_{2;1} + P_{1;2}$	0	$(5.94 \pm 3.43) \cdot 10^{-6}$	$(3.66 \pm 1.38) \cdot 10^{-5}$	$(1.07 \pm 0.76) \cdot 10^{-4}$
$P_{2;2}$	0	0	0	0

TABLE I: List of the photon-number probabilities $P_{n_1;n_2}$ of having n_1 and n_2 photons in the output modes t_1 and t_2 . The events with the same sum of photon numbers in modes t_1 and t_2 are compared to the probability of obtaining one photon in each of the output modes. The error for each probability is following a Poissonian distribution of the measured counts. See Supplementary Information for a more detailed analysis including polarization modes.

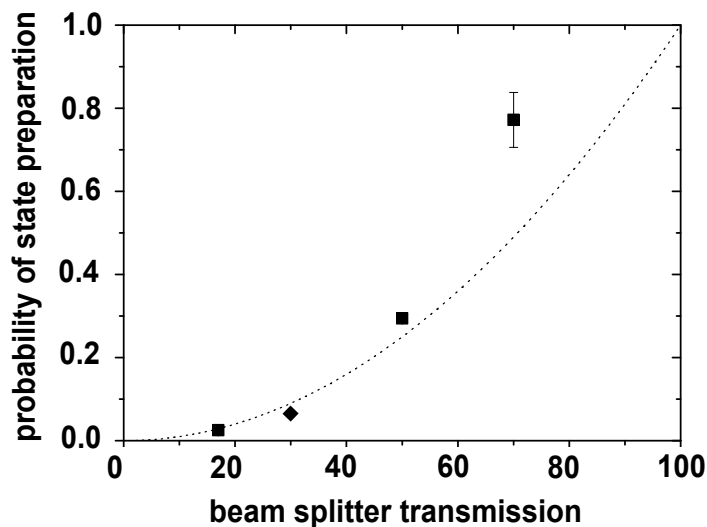


FIG. 2: Probability of heralded entanglement generation shown for various beam splitter transmissions. The deviation from the expected quadratic behavior (line) originates from high-order emissions, which increase the probability of measuring photon pairs in the output modes for higher beam splitter transmissions. The diamond-shaped data point originates from the experiment with the reduced laser-power and the error bars follow a Poissonian statistic.

These probabilities, defined as $P = C_6/(C_4 \cdot \eta^2)$ where C_6 (C_4) is the six(four)-fold coincidence rate and η is the total photon detection efficiency per mode, are $P_{17/83} = (2.5 \pm 0.2)\%$, $P_{50/50} = (29.4 \pm 1.0)\%$ and $P_{70/30} = (77.2 \pm 6.6)\%$ for the different transmission rates. Remarkably, these probabilities are achieved due to the high visibility of $(86.2 \pm 0.7)\%$ for the destructive four-photon quantum interference.

The detection of more than one photon per spatial mode results from eight- or more-photon emissions due to the technical limitation of working in the high laser-power regime for optimizing count rates. Obviously, the detected six-fold coincidences for obtaining the $P_{1,1}$ contribution also capture the higher-order emission, which cover about 10% of the coincidences for the high laser-power case. Naturally, the averaging of correlated and anti- or non-correlated measurement results decreases the quantum correlations of the desired output state. For fair and sensitive representation of this effect an additional set of polarization-correlation measurements is performed. Although these

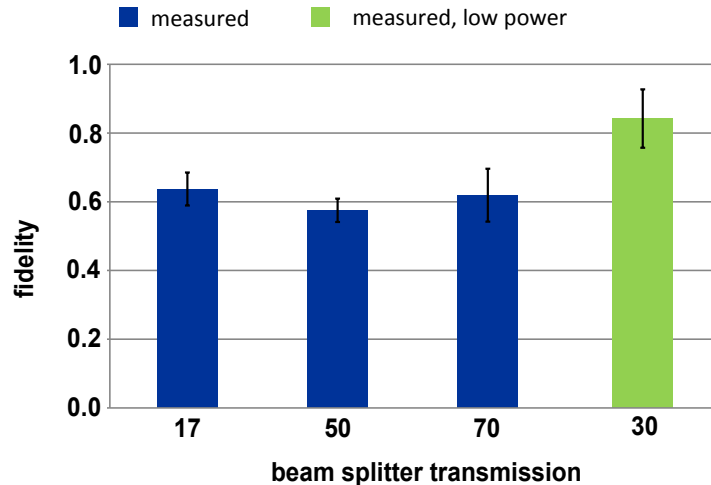


FIG. 3: Experimentally obtained fidelities for the two-qubit polarization state with respect to the ideal state $|\phi^+\rangle$ for various beam splitter transmissions (blue). The effect of higher-order emission is demonstrated by an additional experimental run with a reduced laser-power (green). For this experiment a beam splitter transmission of 30 % is chosen for optimizing the required measurement time. As expected the probability of obtaining the heralded state $|\phi^+\rangle$ increases with the transmittance of the beam splitters, whereas the polarization-state fidelities are not affected. The error bars are derived from Monte Carlo simulations based on a Poissonian distribution of the measured counts.

polarization measurements are triggered by a four-fold coincidence, the requirement of obtaining an additional two-fold coincidence intrinsically leads to a post-selection of the two-photon polarization density matrix (see Figure 4a and Methods). The corresponding fidelity, F^{post} of this measured photon pair with the corresponding entangled quantum state $|\phi^+\rangle$ is $F_{17/83}^{post} = (63.7 \pm 4.9)\%$, $F_{50/50}^{post} = (57.5 \pm 3.4)\%$, and $F_{70/30}^{post} = (61.9 \pm 7.7)\%$ for the different beam splitter ratios via local unitary transformations.

For demonstrating the state fidelities' dependency on the laser-power (Figure 3), an additional experimental run with a reduced laser-power of 620mW and beam splitter transmissions of 30 % was performed. The post-selected density matrix of this state in Figure 4b clearly shows an improvement of the polarization correlations, which is quantified by a fidelity of $F_{30/70}^{post} = (84.2 \pm 8.5)\%$. From this data, we extract the tangle τ [28], a measure of entanglement that ranges from 0 for separable states to 1 for maximally entangled states, as $\tau_{30/70} = 0.55 \pm 0.19$. This density matrix, as commonly written in the coincidence basis, would allow a violation of local realistic theories by almost 2 standard deviations as it implies a maximum Clauser-Horne-Shimony-Holt [29, 30] Bell parameter of $S = 2.36 \pm 0.22$. This laser-power dependent noise is therefore not intrinsic in the setup and is only due to technical limitations, which can be overcome in future experiments by using photon-number discriminating detectors or with high-efficient down-conversion sources.

These two-photon density matrices together with the measured photon number probabilities allow to calculate the state fidelity $F^{meas} = \langle \phi^+ | \rho | \phi^+ \rangle$ of the output state including vacuum and higher-order terms. This measured total state fidelity can be extracted as $F_{17/83}^{meas} = (0.0164 \pm 0.0010)\%$, $F_{30/70}^{meas} = (0.0517 \pm 0.0029)\%$, $F_{50/50}^{meas} = (0.176 \pm 0.013)\%$ and $F_{70/30}^{meas} = (0.497 \pm 0.041)\%$, which have significantly improved to standard down-conversion sources. These results suggest that with future gradual increases to the coincidence rate and the fidelity of entangled photons, the utilization

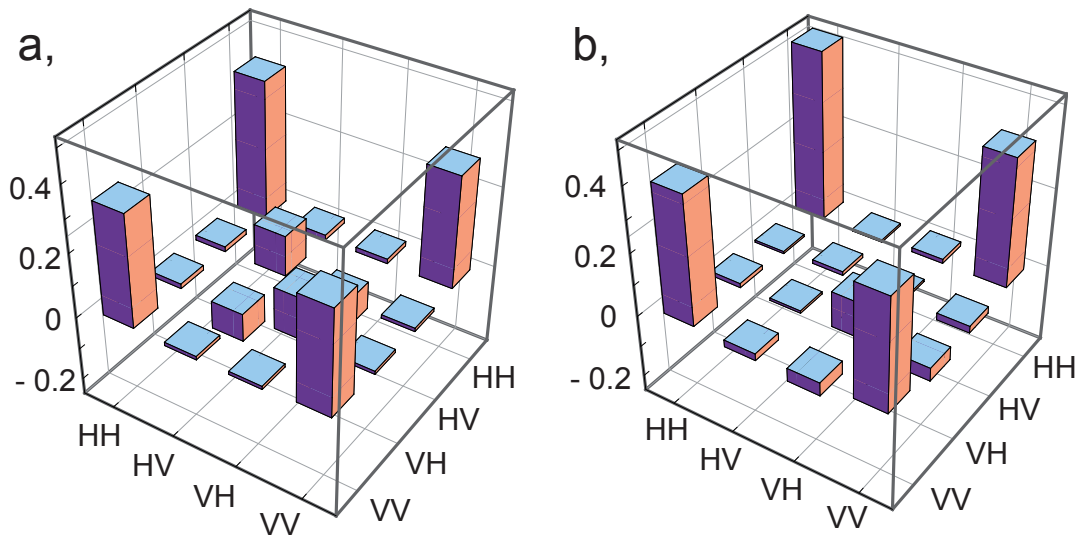


FIG. 4: The effect of higher-order emission for the polarization correlations. The trade-off for the increased coincidence rates is manifested in the contribution of higher-order emission. a, Experimentally obtained polarization density matrix with a laser-power of 1.2 Watt and a beam splitter transmission of 50%. The captured eight-photon contribution leads to a background of a $|\psi^-\rangle$ state. b, The reduction of the background is demonstrated when reducing the laser-power. The experimentally reconstructed two-qubit polarization density matrix is measured with a laser-power of 0.62 Watt and a beam splitter transmission of 30%. The imaginary part of the density matrices is below 0.09 for all elements and hence not shown.

of this scheme for quantum information processing tasks may not be far out of reach.

This experiment presents the first feasible scheme for the generation of heralded entangled photon pairs with SPDC and single-photon detectors. This conditional method achieves a high preparation efficiency of up to 77% with measured fidelities of up to 84% for the post-selected two-photon state. These results successfully underline its potential applicability for entanglement-based technologies. In conclusion, we highlight a multi-photon experiment that generates heralded entangled states as required for long-distance quantum communication and scalable quantum computing. We note that during the course of the work presented here we learned of a parallel experiment by Wagenknecht et al.[31].

The authors are grateful to R. Prevedel, X. Ma, M. Aspelmeyer, Č. Brukner and T. Pittman for discussions and G. Mondl for assistance with the electronics. This work was supported by the Austrian Science Fund (FWF), the Intelligence Advanced Research Projects Activity IARPA under Army Research Office ARO, the European Commission under the Integrated Project Qubit Applications (QAP) and Quantum Interfaces, Sensors, and Communication based on Entanglement (Q-ESSENCE) and the IST directorate, the ERC Senior Grant (QIT4QAD) and the Marie-Curie research training network EMALI.

METHODS

We simultaneously produce six photons in the $|\Psi_3\rangle$ -state by using higher-order emissions of a non-collinear type-II SPDC process. A mode-locked Mira HP Ti:Sa oscillator is pumped by a Coherent Inc. Verdi V-18 laser to reach output powers high enough to be able to exploit third-order SPDC emissions. The pulsed-laser output ($\tau = 200$ fs, $\lambda = 808$ nm, 76 MHz) is frequency-doubled using a 2 mm-thick Lithium triborate (LBO) crystal, resulting in UV pulses of 1.2 W cw average. We achieve a stable source of UV-pulses by translating the LBO with a stepper motor to avoid optical damage to the anti-reflection coating of the crystal (count rate fluctuations less than 3% over 24 h). Afterwards, dichroic mirrors are used to separate the up-converted light from the infrared laser light. The UV beam is focused on a 2 mm-thick β -barium borate (BBO) crystal cut for non-collinear type-II parametric down-conversion. HWPs and additional BBO crystals compensate walk-off effects and allow the production of any Bell state. Narrowband interference filters ($\Delta\lambda = 3$ nm) are used to spatially and spectrally select the down-converted photons which are then coupled into single-mode fibers that guide them to the analyzer setup. There, the photon pairs are directed to non-polarizing beam splitters whose splitting ratios are chosen dependent on the experiment. The reflected modes then are analyzed in $|H/V\rangle$ basis and in $|\pm\rangle$ basis. At this specific angle, where the HWP rotates the polarization by 45° , any possible four-photon state, emitted into the four modes, $r_{1H,1V}$ and $r_{2+,2-}$, will result only in a three-fold coincidence because of $|+-\rangle_{r_2} = (|HH\rangle_{r_2} - |VV\rangle_{r_2})/\sqrt{2}$. Thus, these two photons will never be split up at the PBS and therefore never contribute to a fourfold coincidence detection. The typical photon coupling rates and detector efficiencies for each spatial mode are about 23% and 42%.

Our density matrix is reconstructed by a tomographic set of measurements, where combinations of the single photon projections $|H/V\rangle$, $|\pm\rangle$, and $|R/L\rangle = \frac{1}{\sqrt{2}}(|H\rangle \pm i|V\rangle)$, on each of the two photons in modes t_1 and t_2 are used. The most likely physical density matrix for our 2-qubit state is extracted using a maximum-likelihood reconstruction [25–27]. Uncertainties in quantities extracted from these density matrices are calculated using a Monte Carlo routine and assumed Poissonian errors.

-
- [1] Kwiat, P. G. *et al.* New high-intensity source of polarization-entangled photon pairs. *Phys. Rev. Lett.* **75**, 4337–4341 (1995).
 - [2] Śliwa, C. & Banaszek, K. Conditional preparation of maximal polarization entanglement. *Phys. Rev. A* **67**, 030101 (2003).
 - [3] Nielsen, M. A. & Chuang, I. L. *Quantum Computation and Quantum Information* (Cambridge University Press, 2000).
 - [4] Knill, E., Laflamme, R. & Milburn, G. A scheme for efficient quantum computation with linear optics. *Nature* **409**, 46–52 (2001).
 - [5] Pittman, T., Jacobs, B. & Franson, J. Probabilistic quantum logic operations using polarizing beam splitters. *Phys. Rev. A* **64**, 062311 (2001).
 - [6] O’Brien, J. L., Pryde, G. J., White, A. G., Ralph, T. C. & Branning, D. Demonstration of an all-optical quantum controlled-NOT gate. *Nature* **426**, 264–267 (2003).
 - [7] Pittman, T., Fitch, M., Jacobs, B. & Franson, J. Experimental controlled-NOT logic gate for single photons in the coincidence basis. *Phys. Rev. A* **68**, 032316 (2003).
 - [8] Gasparoni, S., Pan, J.-W., Walther, P., Rudolph, T. & Zeilinger, A. Realization of a photonic controlled-NOT gate

- sufficient for quantum computation. *Phys. Rev. Lett.* **93**, 020504 (2004).
- [9] Kwiat, P., Mitchell, J., Schwindt, P. & White, A. Grover's search algorithm: An optical approach. *J. Mod. Opt.* **47**, 257–266 (2000).
- [10] Prevedel, R. *et al.* High-speed linear optics quantum computing using active feed-forward. *Nature* **445**, 65–69 (2007).
- [11] Tame, M. S. *et al.* Experimental realization of Deutsch's algorithm in a one-way quantum computer. *Phys. Rev. Lett.* **98**, 140501 (2007).
- [12] Lu, C.-Y., Browne, D. E., Yang, T. & Pan, J.-W. Demonstration of a compiled version of Shor's quantum factoring algorithm using photonic qubits. *Phys. Rev. Lett.* **99**, 250504 (2007).
- [13] Lanyon, B. P. *et al.* Experimental demonstration of a compiled version of Shor's algorithm with quantum entanglement. *Phys. Rev. Lett.* **99**, 250505 (2007).
- [14] Walther, P. *et al.* Experimental one-way quantum computing. *Nature* **434**, 169–176 (2005).
- [15] Kimble, H. The quantum internet. *Nature* **453**, 1023–1030 (2008).
- [16] Michler, P. *et al.* A quantum dot single-photon turnstile device. *Science* **290**, 2282–2285 (2000).
- [17] Kurtsiefer, C., Mayer, S., Zarda, P. & Weinfurter, H. Stable solid-state source of single photons. *Phys. Rev. Lett.* **85**, 290–293 (2000).
- [18] Pittman, T. *et al.* Heralded two-photon entanglement from probabilistic quantum logic operations on multiple parametric down-conversion sources. *IEEE J. Sel. Top. Quantum Electron.* **9**, 1478–1482 (2003).
- [19] Walther, P., Aspelmeyer, M. & Zeilinger, A. Heralded generation of multiphoton entanglement. *Phys. Rev. A* **75**, 012313 (2007).
- [20] Kok, P. & Braunstein, S. Limitations on the creation of maximal entanglement. *Phys. Rev. A* **62**, 064301 (2000).
- [21] Zhang, Q. *et al.* Experimental quantum teleportation of a two-qubit composite system. *Nature Phys.* **2**, 678–682 (2006).
- [22] Wieczorek, W. *et al.* Experimental entanglement of a six-photon symmetric Dicke state. *Phys. Rev. Lett.* **103**, 020504 (2009).
- [23] Prevedel, R. *et al.* Experimental Realization of Dicke States of up to Six Qubits for Multiparty Quantum Networking. *Phys. Rev. Lett.* **103**, 020503 (2009).
- [24] Rådmark, M., Zukowski, M. & Bourennane, M. Experimental high fidelity six-photon entangled state for telecloning protocols. *New Journal of Physics* **11**, 103016 (2009).
- [25] James, D., Kwiat, P., Munro, W. & White, A. Measurement of qubits. *Phys. Rev. A* **64**, 052312 (2001).
- [26] Hradil, Z. Quantum-state estimation. *Phys. Rev. A* **55**, R1561–R1564 (1997).
- [27] Banaszek, K., D'Ariano, G. M., Paris, M. G. A. & Sacchi, M. F. Maximum-likelihood estimation of the density matrix. *Phys. Rev. A* **61**, 010304 (1999).
- [28] Coffman, V., Kundu, J. & Wootters, W. K. Distributed entanglement. *Phys. Rev. A* **61**, 052306 (2000).
- [29] Clauser, J. F., Horne, M. A., Shimony, A. & Holt, R. A. Proposed experiment to test local hidden-variable theories. *Phys. Rev. Lett.* **23**, 880–884 (1969).
- [30] Horodecki, R., Horodecki, P. & Horodecki, M. Violating Bell inequality by mixed spin- $\frac{1}{2}$ states: necessary and sufficient condition. *Phys. Lett. A* **200**, 340–344 (1995).
- [31] Wagenknecht, C. *et al.* Experimental Demonstration of a Heralded Entanglement Source. *Nat. Photon.* (in the press).

SUPPLEMENTARY INFORMATION

The analysis of the polarization-dependent photon-number distribution using the Fock basis is shown in Table II. This data represents the diagonal elements of the density matrix, i.e. the probabilities of having n photons in each mode, starting from the vacuum contribution up to the case with one photon in each mode.

	17/83	30/70	50/50	70/30
$P_{0,0,0,0}$	$(9.74 \pm 0.002) \cdot 10^{-1}$	$(9.63 \pm 0.003) \cdot 10^{-1}$	$(9.14 \pm 0.006) \cdot 10^{-1}$	$(8.68 \pm 0.023) \cdot 10^{-1}$
$P_{1,0,0,0}$	$(7.19 \pm 0.08) \cdot 10^{-3}$	$(10.8 \pm 0.15) \cdot 10^{-3}$	$(2.42 \pm 0.04) \cdot 10^{-2}$	$(2.70 \pm 0.12) \cdot 10^{-2}$
$P_{0,1,0,0}$	$(8.32 \pm 0.09) \cdot 10^{-3}$	$(10.2 \pm 0.14) \cdot 10^{-3}$	$(2.26 \pm 0.03) \cdot 10^{-2}$	$(3.25 \pm 0.13) \cdot 10^{-2}$
$P_{0,0,1,0}$	$(5.77 \pm 0.07) \cdot 10^{-3}$	$(8.41 \pm 0.13) \cdot 10^{-3}$	$(1.58 \pm 0.03) \cdot 10^{-2}$	$(2.72 \pm 0.12) \cdot 10^{-2}$
$P_{0,0,0,1}$	$(4.47 \pm 0.65) \cdot 10^{-3}$	$(7.20 \pm 0.12) \cdot 10^{-3}$	$(1.93 \pm 0.03) \cdot 10^{-2}$	$(3.62 \pm 0.14) \cdot 10^{-2}$
$P_{1,1,0,0}$	$(2.08 \pm 0.44) \cdot 10^{-5}$	$(2.38 \pm 0.69) \cdot 10^{-5}$	$(2.41 \pm 0.35) \cdot 10^{-4}$	$(3.75 \pm 1.42) \cdot 10^{-4}$
$P_{1,0,1,0}$	$(12.05 \pm 0.85) \cdot 10^{-5}$	$(32.3 \pm 2.02) \cdot 10^{-5}$	$(10.26 \pm 0.68) \cdot 10^{-4}$	$(2.22 \pm 0.32) \cdot 10^{-3}$
$P_{1,0,0,1}$	$(2.56 \pm 0.73) \cdot 10^{-5}$	$(0.718 \pm 1.63) \cdot 10^{-5}$	$(5.94 \pm 0.64) \cdot 10^{-4}$	$(1.01 \pm 0.33) \cdot 10^{-3}$
$P_{0,1,1,0}$	$(4.88 \pm 0.87) \cdot 10^{-5}$	$(6.84 \pm 1.76) \cdot 10^{-5}$	$(5.22 \pm 0.56) \cdot 10^{-4}$	$(1.83 \pm 0.32) \cdot 10^{-3}$
$P_{0,1,0,1}$	$(6.28 \pm 0.66) \cdot 10^{-5}$	$(21.5 \pm 1.52) \cdot 10^{-5}$	$(9.20 \pm 0.65) \cdot 10^{-4}$	$(2.96 \pm 0.34) \cdot 10^{-3}$
$P_{0,0,1,1}$	$(6.63 \pm 0.25) \cdot 10^{-6}$	$(1.19 \pm 0.49) \cdot 10^{-5}$	$(1.31 \pm 0.26) \cdot 10^{-4}$	$(3.75 \pm 1.42) \cdot 10^{-4}$
$P_{1,1,1,0}$	0	$(1.98 \pm 1.98) \cdot 10^{-6}$	$(2.6 \pm 1.17) \cdot 10^{-5}$	0
$P_{1,1,0,1}$	0	$(3.96 \pm 2.80) \cdot 10^{-6}$	0	$(1.07 \pm 0.76) \cdot 10^{-4}$
$P_{1,0,1,1}$	0	0	$(1.05 \pm 0.74) \cdot 10^{-5}$	0
$P_{0,1,1,1}$	0	0	0	0
$P_{1,1,1,1}$	0	0	0	0

TABLE II: The Table lists the measured probabilities $P_{n_{1H}, n_{1V}; n_{2H}, n_{2V}}$ of finding n_{1H} , n_{1V} , n_{2H} and n_{2V} photons numbers in the output modes t_{1H}, t_{1V}, t_{2H} and t_{2V} with orthogonal polarizations H and V for the different beam splitter transmissions using our standard photo-avalanche diodes. The error for each probability is following a Poissonian distribution of the measured counts.

For each beam splitter transmission ratio we used a (overcomplete) tomographic set of measurements for each basis $\sigma_x, \sigma_y, \sigma_z$ to reconstruct the polarization correlations of the (high-power) output state. In Table III we list the measured detection events that were triggered by a four-fold coincidence of the ancilla photons.

50/50	$\sigma_x^{(1)}\sigma_x^{(2)}$	$\sigma_y^{(1)}\sigma_y^{(2)}$	$\sigma_z^{(1)}\sigma_z^{(2)}$	$\sigma_x^{(1)}\sigma_z^{(2)}$	$\sigma_x^{(1)}\sigma_y^{(2)}$	$\sigma_z^{(1)}\sigma_y^{(2)}$	$\sigma_z^{(1)}\sigma_x^{(2)}$	$\sigma_y^{(1)}\sigma_x^{(2)}$	$\sigma_y^{(1)}\sigma_z^{(2)}$
$ 0, 0; 0, 0\rangle$	32429	15769	16779	14303	14002	16309	31535	17756	15859
$ 1, 0; 0, 0\rangle$	956	443	390	377	387	376	838	446	405
$ 0, 1; 0, 0\rangle$	749	394	482	304	292	443	884	398	374
$ 0, 0; 1, 0\rangle$	576	277	208	204	253	314	623	338	224
$ 0, 0; 0, 1\rangle$	627	319	433	302	292	308	720	312	381
$ 1, 1; 0, 0\rangle$	6	1	9	5	4	5	15	1	0
$ 1, 0; 1, 0\rangle$	47	3	15	13	13	16	29	20	14
$ 1, 0; 0, 1\rangle$	25	38	9	5	14	15	22	12	8
$ 0, 1; 1, 0\rangle$	19	18	8	14	4	8	21	14	7
$ 0, 1; 0, 1\rangle$	33	2	11	17	9	11	48	12	11
$ 0, 0; 1, 1\rangle$	4	1	4	3	0	0	10	2	1
$ 1, 1; 1, 0\rangle$	2	0	0	1	0	0	2	0	0
$ 1, 1; 0, 1\rangle$	0	0	0	0	0	0	0	0	0
$ 1, 0; 1, 1\rangle$	1	0	0	0	0	0	1	0	0
$ 0, 1; 1, 1\rangle$	0	0	0	0	0	0	0	0	0
$ 1, 1; 1, 1\rangle$	0	0	0	0	0	0	0	0	0
70/30	$\sigma_x^{(1)}\sigma_x^{(2)}$	$\sigma_y^{(1)}\sigma_y^{(2)}$	$\sigma_z^{(1)}\sigma_z^{(2)}$	$\sigma_x^{(1)}\sigma_z^{(2)}$	$\sigma_x^{(1)}\sigma_y^{(2)}$	$\sigma_z^{(1)}\sigma_y^{(2)}$	$\sigma_z^{(1)}\sigma_x^{(2)}$	$\sigma_y^{(1)}\sigma_x^{(2)}$	$\sigma_y^{(1)}\sigma_z^{(2)}$
$ 0, 0; 0, 0\rangle$	833	1371	1480	1478	1402	3360	3630	1692	972
$ 1, 0; 0, 0\rangle$	23	55	36	56	52	94	102	64	22
$ 0, 1; 0, 0\rangle$	27	43	79	55	38	136	140	57	33
$ 0, 0; 1, 0\rangle$	26	42	48	31	45	110	121	61	25
$ 0, 0; 0, 1\rangle$	34	47	66	52	44	147	170	76	41
$ 1, 1; 0, 0\rangle$	0	1	1	1	2	2	0	0	0
$ 1, 0; 1, 0\rangle$	4	1	3	3	4	6	6	4	4
$ 1, 0; 0, 1\rangle$	2	5	4	8	4	10	3	3	0
$ 0, 1; 1, 0\rangle$	2	4	2	1	2	11	7	3	4
$ 0, 1; 0, 1\rangle$	4	0	7	1	4	12	6	4	2
$ 0, 0; 1, 1\rangle$	1	0	0	2	2	0	0	2	0
$ 1, 1; 1, 0\rangle$	0	0	0	0	0	0	0	0	0
$ 1, 1; 0, 1\rangle$	0	0	0	0	1	0	1	0	0
$ 1, 0; 1, 1\rangle$	0	0	0	0	0	0	0	0	0
$ 0, 1; 1, 1\rangle$	0	0	0	0	0	0	0	0	0
$ 1, 1; 1, 1\rangle$	0	0	0	0	0	0	0	0	0

TABLE III: We show the measured photon-numbers for each polarization and spatial mode, $|n_{1H}, n_{1V}, n_{2H}, n_{2V}\rangle$, where n_{1H} , n_{1V} denote the photon number for the orthogonal polarization states in output mode 1 and n_{2H} , n_{2V} denote the orthogonal polarization states in output mode 2. The settings for the different measurement bases $\sigma_i^{(1)}\sigma_j^{(2)}$ with $i, j = x, y, z$ are adjusted by phase retarders in front of the polarizing beam splitters.